GENERALIZED COMPLEX ATTRIBUTES AND THEIR USE FOR NMO STRETCHING COMPENSATION

A. VESNAVER[*] and F. POLETTO[*]

Normal Move Out (NMO) correction in the space–time domain is carried out as a time-varying stretching of the seismic trace. The basic limit of this procedure is that early reflections at large offsets are greatly deformed and must be muted before stacking. Although the stack itself can be performed satisfactorily in other domains (such as the f–k), other processing steps such as residual statics require NMO corrected traces. This paper introduces an algorithm able to compensate for NMO stretching. Generalized complex attributes are defined which cast light on various spectral properties of NMO correction. Finally applications to synthetic and real data are discussed.

Keywords: seismic data processing, NMO-correction, seismic attributes, Hilbert transform, envelope, instantaneous phase

1. Introduction

Correction for Normal Move Out (NMO) is the basic preliminary to the stacking of Common Mid Point (CMP) gathers. However, if this operation is performed in the space–time domain, the well-known undesired effect of stretching arises for early reflections at large offsets *(Fig. 1)*. The usual remedy is a surgical mute, which removes the overstretched wavelets and thus reduces the distortion of the stacked signals, but precious information is lost in this way.

Better solutions have been investigated over the last decade, mainly by defining stack procedures in new domains, such as the frequency–wavenumber [GAZDAG and SGUAZZERO 1984]. These new techniques, however, have two major limitations: firstly, they require expensive two-dimensional transforms; secondly, they solve the problem of stacking but not that of NMO correction: in fact, although the summing of coherent signals is the ultimate goal of this procedure, there are numerous processing steps which are executed after NMO correction and before stacking in the space–time domain, such as residual statics, residual NMO, surface consistent deconvolution, mute scans, etc.

In this paper an algorithm is introduced which is able to compensate for NMO stretching based on the concepts of a complex trace [TANER et al. 1979] and phase gain [SGUAZZERO and VESNAVER 1987]. The algorithm requires the definition of new complex attributes generalizing the classical ones, such as instantaneous phase, envelope and instantaneous frequency.

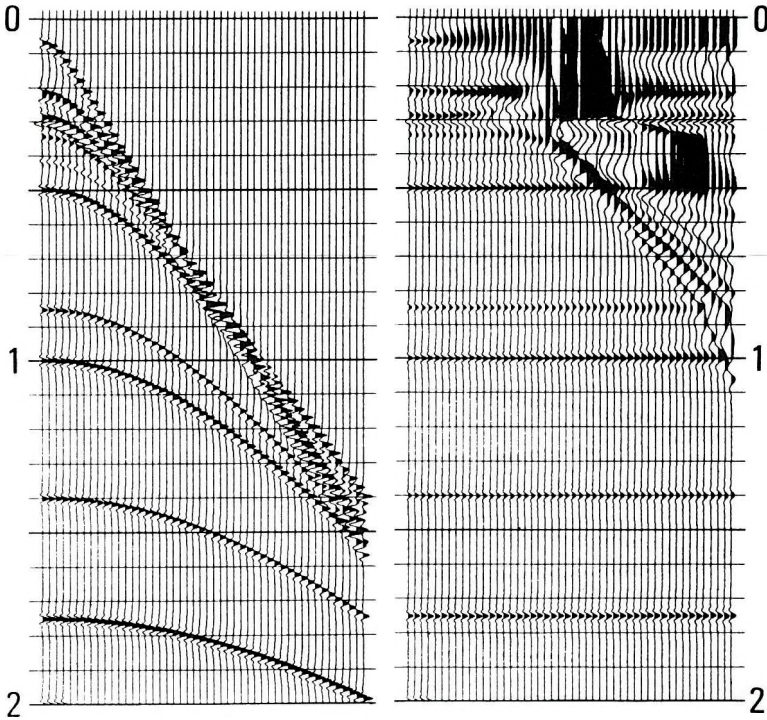[*]Osservatorio Geofisico Sperimentale (OGS), POB 2011, 34016 Trieste, Italy

Fig. 1. Synthetic CMP gather before (left) and after (right) NMO correction

1. ábra. Szintetikus közös középpontos gyűjtés dinamikus korrekció előtt (bal) és után (jobb)

Рис. 1. Синтетический сбор по общей точке до (слева) и после (справа) динамической поправки

2. Generalized complex attributes

Before introducing the proposed algorithm to compensate for NMO stretching, we need to define some old and new attributes of the complex trace.

Definition of attributes

Given a real trace $r(t)$, its corresponding complex trace $c^{(1)}(t)$ is defined as:

$$c^{(1)}(t) = r(t) + i\, \mathbf{H}\{r(t)\} \tag{1}$$

where $\mathbf{H}\{\cdot\}$ indicates the Hilbert transform. We can express in exponential form:

$$c^{(1)}(t) = e^{(1)}(t)\, \exp[i\Phi^{(1)}(t)] \tag{2}$$

where

$$e^{(1)}(t) \equiv |c^{(1)}(t)| \tag{3}$$

and

$$\Phi^{(1)}(t) \equiv \text{Arg}\{c^{(1)}(t)\}$$

Expressions (3) are the definitions of the well-known envelope and instantaneous phase, respectively. They are what we call *first order attributes* in this paper, as emphasized by the superscripts. We can define *second order attributes* as follows.

Envelope $e^{(1)}(t)$ may be regarded as a real-valued trace. So a complex trace $c^{(2)}(t)$ may be defined in a similar way as in (1):

$$c^{(2)}(t) = e^{(1)}(t) + i\mathbf{H}\{e^{(1)}(t)\} = e^{(2)}(t)\exp[i\Phi^{(2)}(t)] \tag{4}$$

where $e^{(2)}(t)$ and $\Phi^{(2)}(t)$ are the second order envelope and instantaneous phase, respectively:

$$e^{(2)}(t) \equiv |c^{(2)}(t)|$$

$$\Phi^{(2)}(t) \equiv \text{Arg}\{c^{(2)}(t)\} \tag{5}$$

i. e. $e^{(2)}(t)$ is the envelope of envelope $e^{(1)}(t)$. Generalizing Eqs. (4) and (5) we obtain:

$$c^{(j+1)}(t) = e^{(j)}(t) + i\mathbf{H}\{e^{(j)}(t)\} = e^{(j+1)}(t)\exp[i\Phi^{(j+1)}(t)]$$

$$e^{(j)}(t) \equiv |c^{(j)}(t)|$$

$$\Phi^{(j)}(t) \equiv \text{Arg}\{c^{(j)}(t)\} \tag{6}$$

These recursions, together with Eq. (1), define the *generalized complex attributes* of the real trace $r(t)$.

Figure 2 displays a simple synthetic trace composed of two zero-phase waveforms of opposite polarity. The first order envelope and instantaneous phase are superimposed. We notice that where there is the main lobe of the positive wavelet, the instantaneous phase is close to zero, while in correspondence to the main lobe of the negative wavelet the phase is discontinuous. This fact will be considered again later.

Figure 3 shows higher order envelopes of the same data. When the envelope order increases, the curves are smoother, particularly near the envelope maxima, i. e. where the signal energy is significant. *Figure 4* shows higher order instantaneous phases of these data. We notice two relevant features: firstly, all

curves intersect each other approximately where there are the two maxima of the envelopes in Figure 2; secondly, in proximity to these intersection points the curves display a linear trend.

Higher order complex attributes have been introduced principally for their mathematical usefulness (as shown in the following paragraph), but they do not seem to have immediate physical significance. Nevertheless, we can emphasize that they share the basic properties of first order complex attributes, due to the nature itself of the Hilbert transform; in particular, any value of the computed complex trace depends on all values of the real trace, and not only on the single value at the corresponding arrival time. This characteristic allows the physical continuity of the whole wave propagation phenomenon to be comprised in the algorithms based on complex traces, exploiting the information redundancy in the data, which redundancy is due to the physical constraints obeyed by the data.
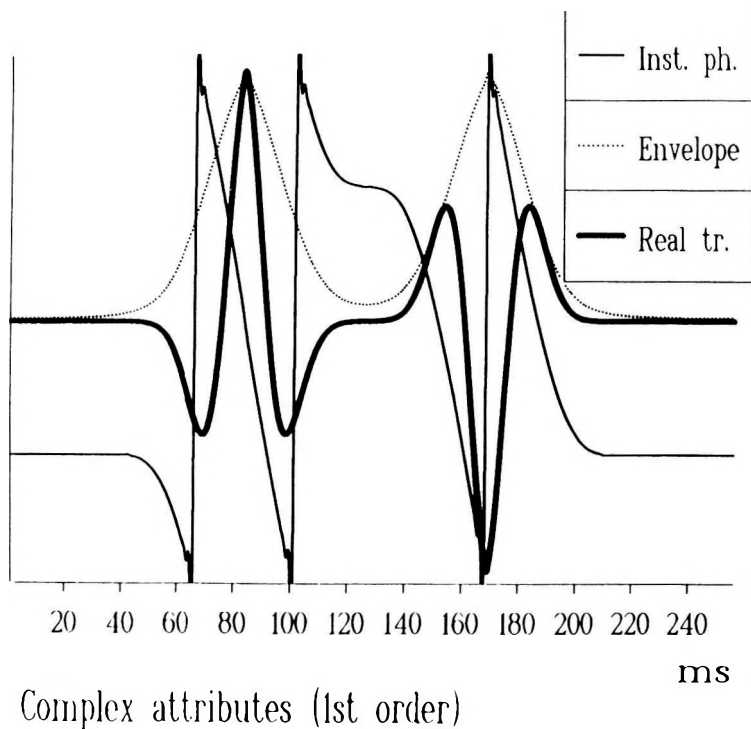

Complex attributes (1st order)

Fig. 2. First order complex attributes of a simple synthetic trace (heavy solid line): envelope (dotted line) and instantaneous phase (solid line)

2. ábra. Szintetikus szeizmogram (vastag vonal) elsőfokú komplex attributumai: burkoló (pontozott) és pillanatnyi fázis (folyamatos vonal)

Рис. 2. Комплексные характеристики первого порядка синтетической сейсмограммы (жирная линия): объемлющая (точки) и мгновенная фаза (сплошная)
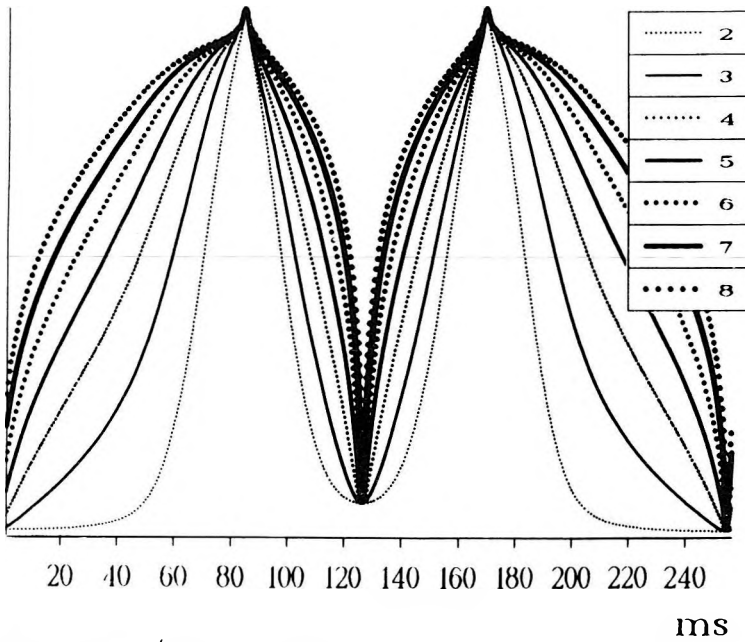
Envelope (2nd to 8th order)

Fig. 3. Second to eighth order envelopes of the trace in Fig. 2

3. ábra. Szintetikus szeizmogram (2. ábra) burkolója (másodfokútól nyolcadfokú közelítésig)

Рис. 3. Обьемлющая (приближения от второго до восьмого порядка) синтетической сеймограммы (рис. 2)

Complex trace expansion

We are going now to use these generalized complex attributes to express the real trace $r(t)$ in a suitable form to compensate for NMO stretching. From definitions (1) and (2) it follows that:
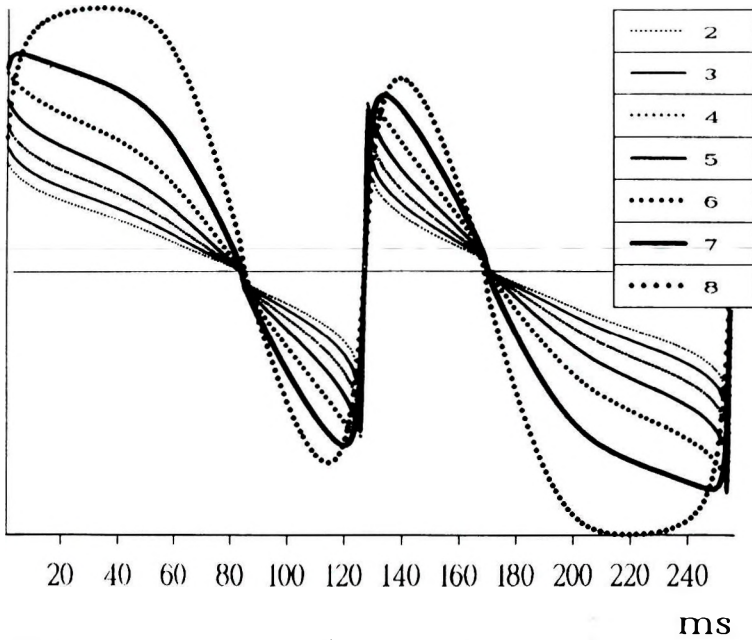
$$r(t) = \text{Re}\{c^{(1)}(t)\} = e^{(1)}(t) \cos[\Phi^{(1)}(t)] \tag{7}$$

Similarly:

$$e^{(1)}(t) = \text{Re}\{c^{(2)}(t)\} = e^{(2)}(t) \cos[\Phi^{(2)}(t)] \tag{8}$$

Substituting $e^{(1)}(t)$ in (7) using (8) we get:

$$r(t) = e^{(2)}(t) \cos[\Phi^{(2)}(t)] \cos[\Phi^{(1)}(t)] \tag{9}$$

Instantaneous phase (2nd to 8th order)

Fig. 4. Second to eighth order instantaneous phases of the trace in Fig. 2

4. ábra. Szintetikus szeizmogram (2. ábra) pillanatnyi fázisa (másodfokútól nyolcadfokú közelítésig)

Рис. 4. Мгновенная фаза (приближения от второго до восьмого порядка) синтетической сейсмограммы (рис. 2)

Substituting iteratively envelopes $e^{(j)}(t)$ in Eq. (9) using recursions Eq. (6) we finally obtain:

$$r(t) = e^{(N)}(t) \cos[\Phi^{(N)}(t)] \cos[\Phi^{(N-1)}(t)] \ldots \cos[\Phi^{(1)}(t)] \tag{10}$$

where N is an arbitrary integer number. If N is relatively large, the N-th order envelope $e^{(N)}(t)$ is relatively smooth where the energy of $r(t)$ is significant. So the main value of Eq. (10) is that most information is contained in the generalized instantaneous phases $\Phi^{(j)}(t)$.

We can now expand the $\Phi^{(j)}(t)$ functions by a first order Taylor series:

$$\Phi^{(j)}(t) \approx \Phi^{(j)}(\tilde{t}) + (t - \tilde{t})\frac{\mathrm{d}}{\mathrm{d}t}[\Phi^{(j)}(t)]_{t=\tilde{t}} = \Phi^{(j)}(\tilde{t}) + \tau\Gamma^{(j)}(\tilde{t}) \tag{11}$$

where $\tilde{t}$ is an arbitrary arrival time, and $\Gamma^{(j)}(t)$ is the j-th order *instantaneous frequency:*

$$\Gamma^{(j)}(t) = \frac{\mathrm{d}}{\mathrm{d}t}[\Phi^{(j)}(t)] \tag{12}$$

If $\tilde{t}$ is chosen as the time of the maximum of the positive zero-phase wavelet, then $\Phi^{(j)}(\tilde{t})$ is close to zero and equation (11) is simplified:

$$\Phi^{(j)}(t) \approx \tau \, \Gamma^{(j)}(\tilde{t}) \tag{13}$$

At minima of negative zero-phase wavelets, for the first order function the following relation holds:

$$\Phi^{(1)}(t) \approx \pi + \tau \, \Gamma^{(1)}(\tilde{t}) \tag{14}$$

but by removing the *apparent polarity* (see Appendix A) we obtain that all instantaneous phases $\Phi^{(j)}(t)$ of all wavelets in the seismogram $r(t)$ may be expanded as in Eq. (13). However, we will have to restore the initial apparent polarity as the last step in the procedure we are defining.

Substituting Eq. (13) into Eq. (10) we can finally express the seismic trace $r(t)$ as follows:

$$r(t) = e^{(N)}(t)\prod_{j=1}^{N}\cos[\Phi^{(j)}(t)] \approx e^{(N)}(t)\prod_{j=1}^{N}\cos[\tau\Gamma^{(j)}(\tilde{t})] \tag{15}$$

Equation (15) is in a very convenient form to apply NMO-stretching compensation.

3. NMO stretching description

The NMO stretching effect was described by DUNKIN and LEVIN [1973]. Since their equations provide the basis for this paper, we recall briefly their results in this section.

Time domain

The arrival time t_x of a signal from a given reflector is a function of the offset x between source and receiver. If we assume that the earth is horizontally layered, this function is the well known Move Out hyperbola:

$$t_x = [t_0 + x^2/v^2(t_0)]^{1/2} \tag{16}$$

where $v(t_0)$ is the stacking velocity at zero-offset time, t_0. In particular, equation (16) relates the arrival time t_x of the signal recorded at offset x with t_0, which is the arrival time of the same signal after NMO correction, when all reflections from the same reflecting point are moved to zero offset.

Expanding $t_0 = t_0(t_x)$ by a Taylor series of the first order, we may express t_0 as a linear function of t_x:

$$t_0 \approx \tilde{t}_0 + [t_x - \tilde{t}_x][dt_0/dt_x] \qquad (17)$$

where:

$$\frac{dt_0}{dt_x} = \frac{\tilde{t}_x}{\tilde{t}_0} \frac{1}{\{1 - [x^2/(\tilde{t}_0 \, v^3)] \, dv(\tilde{t}_0)/dt_0\}} = \sigma \qquad (18)$$

$$\tilde{t}_x = [\tilde{t}_0^2 + x^2/v^2(\tilde{t}_0)]^{\frac{1}{2}} \qquad (19)$$

We denote by $\tilde{t}_x$ the origin of the Taylor series expansion at the wavelet centre in a trace with offset x *(Fig. 5)*, and σ is a stretching factor greater than 1, which depends on offset, time, stacking velocity and its time derivative: $\sigma = \sigma(x, t_0, v(t_0), dv(t_0)/dt_0)$. Manipulating Eq. (17) and substituting Eq. (18) we have:

$$\tau_0 = t_0 - \tilde{t}_0 \approx \sigma[t_x - \tilde{t}_x] = \sigma \tau_x \qquad (20)$$

The variable τ_x is the *local time* in the reference frame of the series expansion at offset x. Equation (20) means that, within a first order approximation, *NMO correction is a local time expansion*. In fact, if Dt_0 and Dt_x are the sampling intervals at offset 0 and x, then from (20) we get:

$$Dt_0 = \sigma Dt_x \qquad (21)$$

Equation (21) emphasizes that NMO correction requires a time-varying sampling of traces at offset x. The values sampled at offsets x from an irregular hyperbolic grid are then translated into a different regular grid at offset 0 *(Fig. 6)*.

Frequency domain

Some simple relations between wavelet spectra before and after NMO stretching may be demonstrated in the frequency domain. If f_0 and f_x are the local frequencies associated with local times τ_0 and τ_x, we get from Eq. (20):

$$f_0 = 1 / \tau_0 = 1 / (\sigma \tau_x) = f_x / \sigma \tag{22}$$

Furthermore, since NMO correction changes the shape but not the amplitudes of the waveform w_x, then:

$$w_0(\tau_0) = w_x(\tau_x) \tag{23}$$

Substituting (20) in (23), we obtain:

$$w_0(\tau_0) = w_x(\tau_0 / \sigma) \tag{24}$$

Exploiting the shift-theorem and using Eqs. (20) to (24), we get finally:

$$W_0(f_0) = \sigma \, W_x(\sigma f_0) = \sigma \, W_x(f_x) \tag{25}$$

Equations (22) and (25) mean that NMO stretching produces a scaling of the waveform spectrum and a remapping of frequencies into lower bands, since $\sigma \geq 1$.
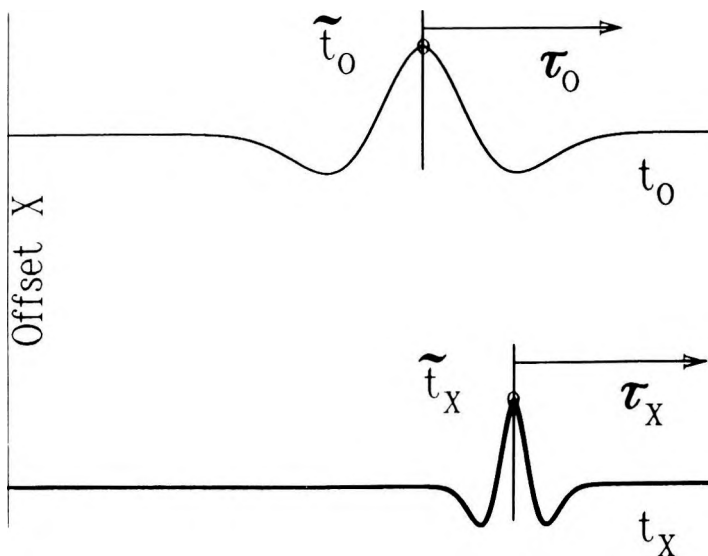

Fig. 5. Zero-phase wavelet at offset x (lower part) is converted to offset 0 by NMO correction (upper part). The stretching effect is evident

5. *ábra. x* észlelési távolságú elemi jel (alul) és ennek dinamikus korrekció utáni alakja (felül). A nyújtó hatás egyértelműen látszik

Рис. 5. Элементарный сигнал (внизу) и ее вид после динамической поправки (вверху) при расстоянии *x* между источником и приемником. Однозначно отмечается эффект удлинения
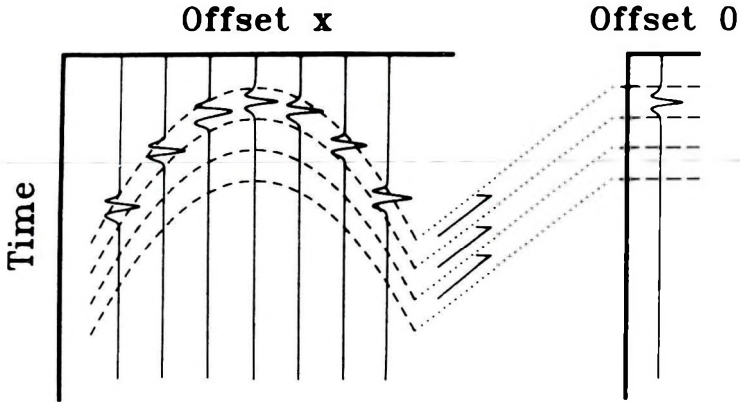
Fig. 6. Time varying sampling of a trace at offset *x* mapped to offset 0

6. *ábra.* *x* észlelési távolságú csatorna időben változó mintavételezésének transzformálása 0 észlelési távolságra

Рис. 6. Приведение дискретности, переменной во времени, трассы с расстоянием *x* между источником и приемником к расстоянию 0 между источником и приемником

4. NMO stretching compensation

Mathematical formulation

NMO stretching compensation may be performed as a correction for wavelet spectrum compression in the frequency domain — (as described above in Eq. (25)). To this end, we recall the definition of instantaneous spectrum $S_x(t_x, f_x)$ [e. g. ACKROYD 1970]:

$$S_x(t_x, f_x) = r_x(t_x) R_x^*(f_x) \exp(-2\pi i f_x t_x) \tag{26}$$

where the asterisk indicates a conjugation. A useful expression relating the first moment of the instantaneous spectrum $S_x(t_x, f_x)$ (i. e., its centroid abscissa) and instantaneous frequency $\Gamma_x(t_x)$ can be demonstrated:

$$\Gamma_x(t_x) = \text{Re} \left| \frac{\int\limits_{-\infty}^{\infty} f_x \, S_x(t_x, f_x) \, df_x}{\int\limits_{-\infty}^{\infty} S_x(t_x, f_x) \, df_x} \right| \tag{27}$$

Using (20), (22), (23) and (25), we get:

$$\Gamma_x(t_x) = \text{Re} \left| \frac{\int\limits_{-\infty}^{\infty} \sigma f_0 \, S_0(t_0, f_0) \, df_0}{\int\limits_{-\infty}^{\infty} S_0(t_0, f_0) \, df_0} \right| = \sigma \, \Gamma_0(t_0) \tag{28}$$

which also expresses the shift of the instantaneous spectrum centroid towards a lower frequency due to NMO correction. To move the centroid back towards its original frequency, we have to multiply $\Gamma_0(t_0)$ by σ:

$$\bar{\Gamma}_0(t_0) = \sigma \, \Gamma_0(t_0) \tag{29}$$

obtaining in this way the NMO-stretching compensated instantaneous frequency $\bar{\Gamma}_0(t_0)$.

In equations (26) to (29) we dropped the superscript indicating the order of the complex attributes to simplify the notation, but the result expressed by (29) holds for any order of instantaneous frequency $\Gamma_0^{(j)}(t_0)$. Therefore, the seismic trace $\bar{r}_0(t)$ after NMO correction and stretching compensation is given by:

$$\bar{r}_0(t) \approx e_0^{(N)}(t) \prod_{j=1}^{N} \cos[\sigma \, \tau \, \Gamma_0^{(j)}(\bar{t})] \approx e_0^{(N)}(t) \prod_{j=1}^{N} \cos[\sigma \, \Phi_0^{(j)}(t)] \tag{30}$$

which is obtained from (15) simply by scaling the generalized instantaneous phases $\Phi^{(j)}(t)$ or frequencies $\Gamma^{(j)}(t)$ by the σ factor, according to Eqs. (13) and (29). We may call this scaling N-th order phase gain, since it generalizes a similar procedure introduced by SGUAZZERO and VESNAVER [1987] to enhance the sharpness of velocity spectra.

Spectral interpretation

We saw previously that NMO stretching produces a remapping of the trace spectrum towards lower frequencies. This effect is sketched in *Fig. 7*, together with that of its compensation by phase gain. We see that a boxcar spectrum of a

wavelet at offset x (part A) is scaled, shifted and compressed by NMO correction to offset 0 (part B). A first order phase gain compensation for NMO stretching (part C) shifts the spectrum back to its initial position, but does not restore the initial bandwidth (see Appendix B).

Better results are obtained if a higher order phase gain is used. In fact, we may separate the factors of $\bar{r}_0(t)$ in Eq. (30) into two classes. In the first one, there are the N cosinusoidal waves $\cos[\sigma\Phi_0^{(j)}(t)]$. Since their spectra are spikes instead of bands, they are accurately compensated for NMO stretching by phase gain. On the other hand, envelope $e_0^{(N)}(t)$ may be regarded as an uncompensated component. Nevertheless, if order N is not too small, $e_0^{(N)}(t)$ is a smooth curve which is not very sensitive to stretching residuals.

Figure 8 displays the effect of phase gain of increasing order on the wavelets of Fig. 2, using a constant gain factor $\sigma = 1.4$. The increasing accuracy obtained in waveform preservation is evident especially in the first three orders. If N is greater than 3 only marginal improvements are obtained.
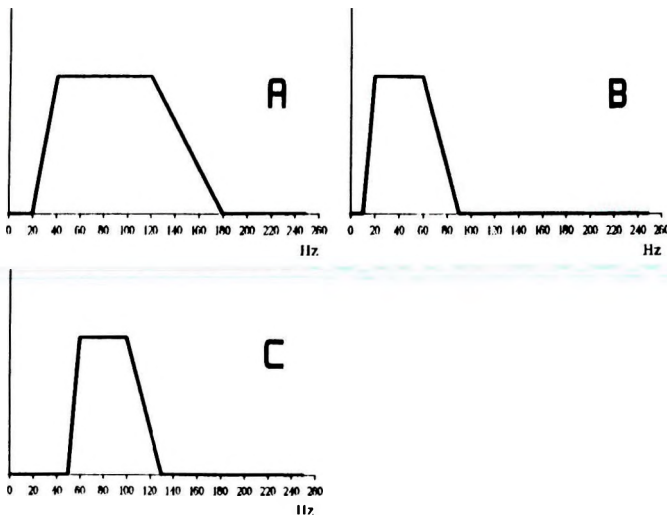

Fig. 7. Band-limited flat spectrum of a wavelet at offset x (part A) undergoes NMO correction to offset 0 (part B). A first order phase gain compensation for NMO stretching (part C) restores the initial position of the spectrum, but not its original bandwidth

7. ábra. x észlelési távolságú elemi jel sávkorlátozott spektruma (A), a dinamikus korrekció okozta spektrumváltozás (B) és ez elsőfokú fáziserősítés-kompenzáció után (C). A nyújtóhatás kompenzálása helyreállítja a spektrum eredeti helyzetét, de sávszélességét nem

Рис. 7. Ограниченный по частоте спектр элементарного сигнала при расстоянии x между источником и приемником (А), изменение спектра, вызванное динамичеcкой поправкой (В), и то же после компенсирования усиления фаз первой ступени (С). Компенсированнем эффекта удлинения восстанавливается исходное положение спектра, но не восстанавливается ширина полос
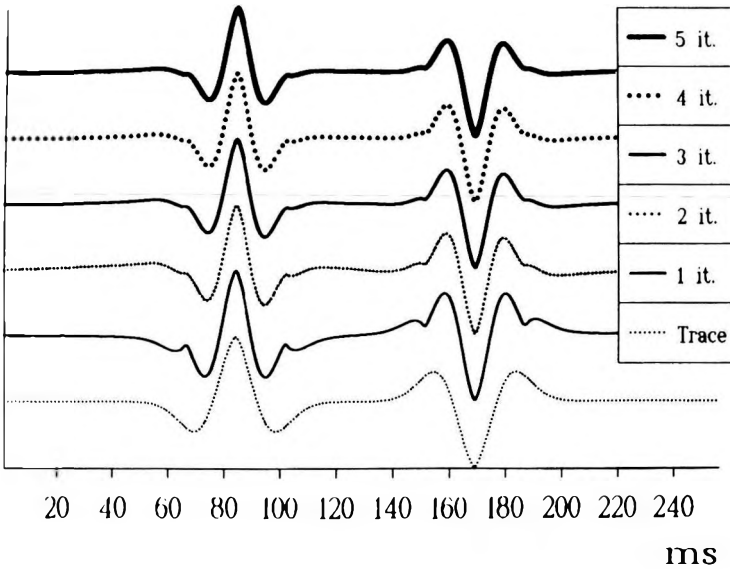
Fig. 8. Effect of phase gain of increasing order to compress the wavelets in Fig. 2.
The σ value is 1.4

8. ábra. A 2. ábra szintetikus szeizmogramja elemi jeleinek összenyomása növekvő fokú
fáziserősítéssel (σ=1,4)

Рис. 8. Сжатие элементарных сигналов синтетической сейсмограммы рис. 2 при нарастающем
усилении фаз (σ = 1,4)

5. Application to synthetic and real data

The synthetic CMP gather in Fig. 1 was generated by convolving a zero-phase wavelet with a reflectivity series simulating primary reflections from horizontal layers, and therefore obeying the hyperbolic Move Out law (Eq. (16)). The sampling rate is 2 ms, the offset range from 0 to 2350 m, the spacing of traces is 50 m.

Figure 9 displays the effect of NMO stretching compensation on the data in Fig. 1 using two different orders for the phase gain, i. e. 1 (part B) and 3 (part C). Obviously, the overstretched wavelets were recompressed only within certain limits, so that the need for a mute is not eliminated, but simply reduced. Later some incoherent band-limited noise is added and mute scans are carried out on a group of CMP gathers of the same model.
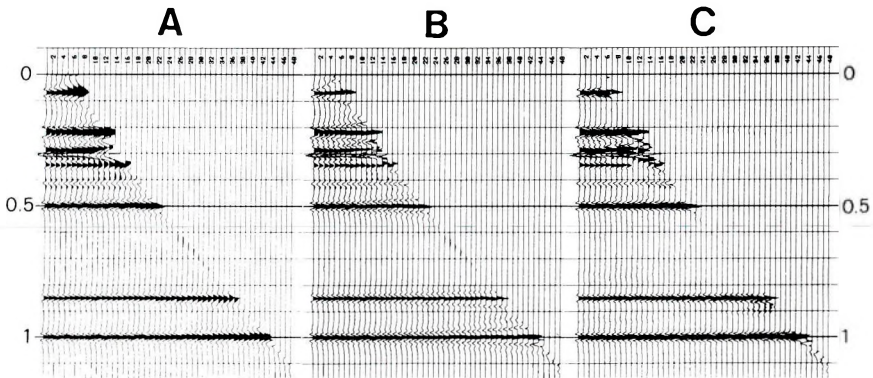
Fig. 9. NMO stretching compensation of the muted data in Fig. 1 using A) input data;   B) using phase gain, $N=1$;   C) using phase gain, $N=3$

9. ábra. A dinamikus korrekció nyújtó hatásának kompenzálása az 1. ábra vágás utáni adatain
A) bemenő adatok; B) fáziserősítés, $N=1$;
C) fáziserősítés, $N=3$

Рис. 9. Компенсирование эффекта удлинения от динамической поправки на данных рис. 1 после срезания
А) Входные данные; В) Усиление фаз, $N = 1$; С) Усиление фаз, $N = 3$

In *Figures 10* and *11* we can compare the results obtained by standard NMO correction with those obtained using phase gain compensation. An increasing abscissa corresponds to an increasing number of near offset traces added to the stack. We notice that NMO stretching compensation not only allows the choice of a much wider mute at any given arrival time, but also improves the high frequency content of the stacked signals. A by-product of these effects is that incoherent noise is damped much more since a wider mute is used, so that an additional improvement of the signal to noise ratio is achieved.

Figures 12 and *13* display mute scans of marine data, acquired by OGS in the Mediterranean Sea. The sampling rate is 4 ms, the maximum fold is 12 and the offset range is between 220 and 2620 m. We notice that by compensating for NMO stretching (Fig. 13) a sharp water bottom reflection is obtained for any fold, whilst without this compensation other high frequency signals appear distorted in Fig. 12.

Figures 14 and *15* show the effectiveness of stretching compensation on a stacked seismic section from the same dataset as Figs 12 and 13. Once more, we see that the compensated stack (Fig. 15) improves the resolution of the uppermost reflections, whilst in the lower part, where the stretching effects are negligible, the two sections are almost identical.
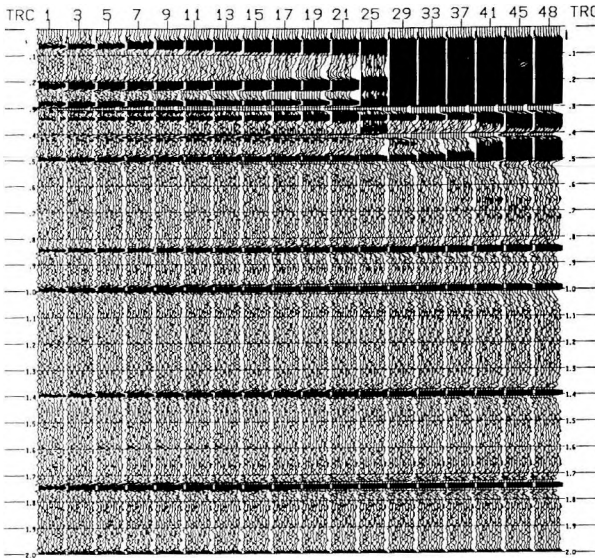
Fig. 10. Mute scan on synthetic data using standard processing

10. ábra. Vágás vizsgálat szintetikus adatokon, hagyományos feldolgozás mellett

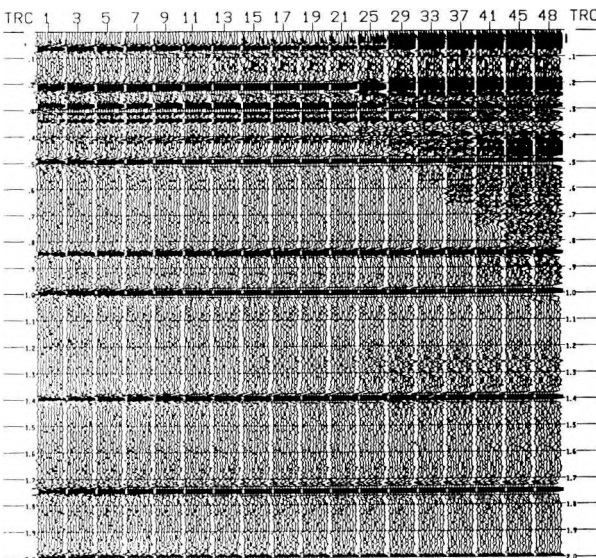*Рис. 10.* Исследование срезания на синтетических данных при традиционной обработка

Fig. 11. Mute scan on the same data as in Fig. 10 using NMO stretching compensation

11. ábra. Vágás vizsgálat a 10. ábra adatain, a dinamikus korrekció nyújtó hatásának kompenzálásával

Рис. 11. Исследование срезания на данных рис. 10 при компенсировании эффекта удлинения от динамической поправки
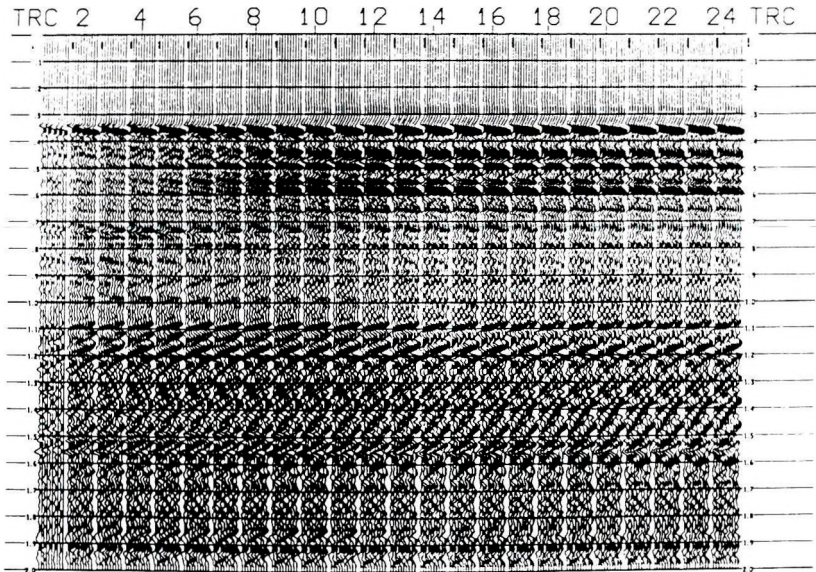
Fig. 12. Mute scan on real marine data using standard processing

12. ábra. Vágás vizsgálat tengeri adatokon, hagyományos feldolgozás mellett

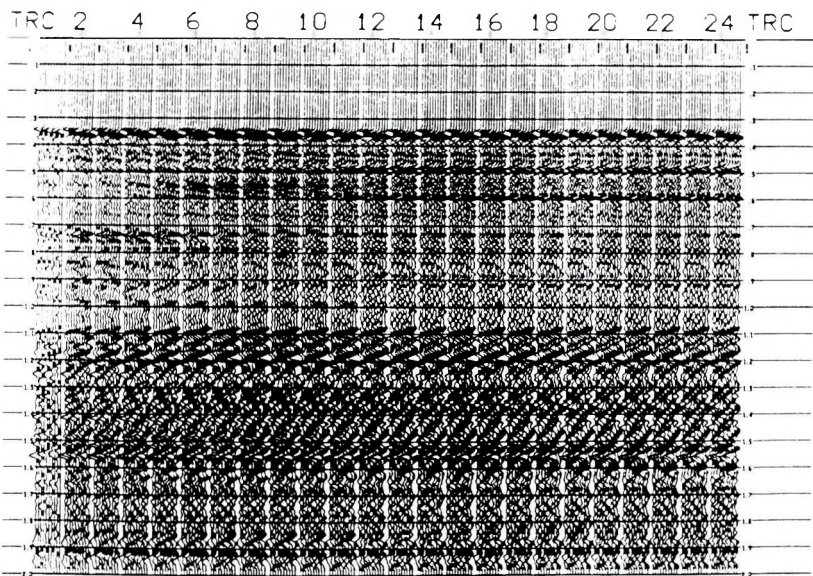Рис. 12. Исследование срезания на морских при традиционной обработке

Fig. 13. Mute scan on the same data as in Fig. 12 using NMO stretching compensation

13. ábra. Vágás vizsgálat a 12. ábra adatain, a dinamikus korrekció nyújtó hatásának kompenzálásával

Рис. 13. Исследование срезания на данных рис. 12 при компенсировании эффекта удлинения от динамической поправки
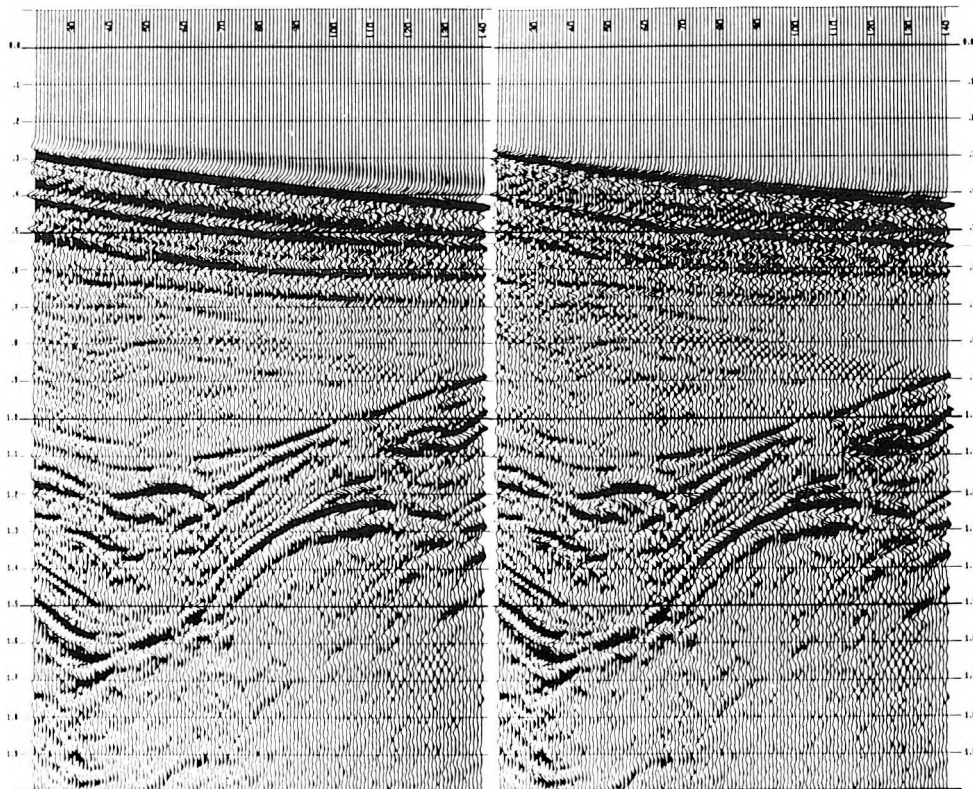
Fig. 14. Stacked seismic section obtained
by standard processing

14. ábra. Hagyományos feldolgozással
készült összegszelvény

Рис. 14. Суммированный разрез,
полученный при традиционной
обработке

Fig. 15. The same stacked section as in
Fig. 14 using NMO stretching
compensation

15. ábra. A 14. ábra szelvénye a
dinamikus korrekció nyújtó hatásának
kompenzálásával

Рис. 15. Разрез рис. 14 при
компенсировании эффекта удлинения
от динамической поправки

6. Conclusions

An algorithm able to reduce NMO stretching artifacts has been introduced, it is based on trace factorization using generalized complex attributes. Improvements are obtained for near-surface reflections, in particular for offsets which are large with respect to reflector depths. For this reason, the procedure is useful if the exploration target is the uppermost layers, i. e. for high resolution surveys.

From the computational point of view, NMO stretching compensation is neither cheap nor expensive. The operation number required for each order of phase gain is slightly higher than for linear filtering; since second or third order algorithms are satisfactory, it follows that the global cost is about three times that of pre-stack linear filtering. However, it should be emphasized that vector or parallel computer architecture may significantly reduce the computational impact. In fact, all operations required are typically of vector type and, since the traces are considered independently, they may be shared amongst different processors.

Acknowledgements

Appendix A

In their classic paper, TANER et al. [1979] define apparent polarity as the sign of the seismic trace $r(t)$ when its envelope $e^{(1)}(t)$ has local maxima. Since we need to associate apparent polarity with a whole wavelet instead of with a few points, we extend the definition by the following algorithm:

— compute envelope $e^{(1)}(t)$;

— delimit the lobes of envelope $e^{(1)}(t)$ as the parts comprised between two consecutive relative minima;

— assign to all samples within a lobe the sign of trace $r(t)$ at the maximum of the envelope in that lobe.

To remove the apparent polarity we have to multiply $r(t)$ by the step-wise sequence so obtained. To restore the initial polarity, the data are multiplied once more by the apparent polarity function of $r(t)$.

Appendix B

Let us consider a zero-phase wavelet $w(t)$ whose spectrum $W(f)$ is the following boxcar function:

$$W(f) = 1, \text{ for: } |f_c - Df| \le |f| \le |f_c + Df|$$

$$= 0, \text{ elsewhere} \qquad (B\text{-}1)$$

where f_c is the central frequency and Df is the half-width of the frequency band (Fig. 7). Wavelet $w(t)$ is given by:

$$w(t) = [\sin(f_c + Df)t - \sin(f_c - Df)t] / [\pi t] \tag{B-2}$$

whilst its complex counterpart $c^{(1)}(t)$ is:

$$c^{(1)}(t) = \exp(\mathrm{i}\, f_c t) \sin(Df\, t) / [\pi t] \tag{B-3}$$

In this case, the central frequency f_c coincides with the instantaneous frequency. Applying a first order phase gain implies a multiplication of f_c by the stretching factor σ, but this is nothing other than a translation of the frequency band because its half-width Df remains unchanged (Fig. 7).

REFERENCES

ACKROYD M. H. 1970: Instantaneous spectra and instantaneous frequency. Proceedings IEEE **58**, 141 p.

DUNKIN J. W. and LEVIN F. K. 1973: Effect of Normal Move Out on a seismic pulse. Geophysics **38**, 4, pp. 635–642

GAZDAG J. and SGUAZZERO P. 1984: Interval velocity analysis by wave extrapolation. Geophysical Prospecting **32**, 3, pp. 454–479

SGUAZZERO P. and VESNAVER A. 1987: A comparative analysis of algorithms for stacking velocity estimation. In: Deconvolution and Inversion, Bernabini et al. (eds), Blackwell, pp. 267–286

TANER M. T., KOEHLER F. and SHERIFF R. E. 1979: Complex seismic trace analysis. Geophysics **44**, 6, pp. 1041–1063

ÁLTALÁNOSÍTOTT KOMPLEX ATTRIBUTUMOK ÉS ALKALMAZÁSUK A DINAMIKUS KORREKCIÓ NYÚJTÓ HATÁSÁNAK KOMPENZÁLÁSÁRA

A. VESNAVER és F. POLETTO

Az NMO-korrekció a tér–idő tartományban lényegében a szeizmikus csatornák időben változó nyújtása. A művelet alapvető korlátja a korai, nagy észlelési távolságú reflexiók erős deformálódása. Ezért ezeket stacking előtt kivágják. Noha maga a stack egyéb tartományokban (pl. *f–k* tartományban) torzítás nélkül elvégezhető, egyéb feldolgozási lépésekhez, mint pl. a maradék statikus korrekcióhoz NMO-korrigált csatornák szükségesek. A dolgozatban egy olyan algoritmust mutatnak be, amely képes kompenzálni az NMO-korrekció nyújtó hatását. Általánosított komplex attributumokat vezetnek be, amelyek rávilágítanak az NMO-korrekció spektrális tulajdonságaira. Végül szintetikus és valódi adatokon szemléltetik az eljárás alkalmazhatóságát.

ОБОБЩЕННЫЕ КОМПЛЕКСНЫЕ ХАРАКТЕРИСТИКИ И ИХ ПРИМЕНЕНИЕ В КОМПЕНСИРОВАНИИ ЭФФЕКТА УДЛИНЕНИЯ ОТ ДИНАМИЧЕСКОЙ ПОПРАВКИ

А. ВЕСНАВЕР и Ф. ПОЛЕТТО

Динамическая поправка в пространственно-временной области по существу означает переменное во времени удлинение сейсмических трасс. Фундаментальным ограничением метода является сильная деформация ранних отражений при больших растояниях между источником и приемником. Поэтому эти отражения удаляются перед суммированием. Хотя само суммирование в других областях, например, в области $f–k$, может быть выполнено без искажений, для других ступеней обработки, как например, для остаточной статической поправки, необходимы трассы с динамической поправкой. В работе представляется алгоритм, благодаря которому становится возможным компенсирование удлиняющего эффекта от динамической поправки. Вводятся обобщающие комплексные характеристики, относящиеся к спектральным особенностям динамической поправки. Наконец, на синтетических и реальных данных иллюстрируется применение способа.